CHAPTER 3: EXPERIMENTAL VERIFICATION: SCALED WATER MODEL AND RESULTS

The importance of a correct CFD model is immeasurable, as an incorrect model (non-repeatable solutions) will render the entire design optimisation process useless. At first, this study was based on the assumption that the CFD models are physically correct and that repeatable results will easily be obtained. However, it was soon discovered that the specific flow situation (jet flowing into a bigger cavity) is complicated and that experimental verification is essential to ensure correct CFD models. Thus, it was decided that a water model should be built to verify the CFD models of the base case Submerged Entry Nozzle (SEN) design (and obviously later designs as well).

A full-scale water model simplifies the comparison of results with the plant circumstances due to the similar kinematic viscosities[1] of water and steel. However, the water model is a 40%-scaled model due to height constraints in the university laboratory. An equivalent full-scale height of 3 to 4 metres is achieved with the 40%-scaled model, which the author deems as a necessity to prevent effects of the bottom on the flow field (which would have been the case with a shallower full-scale water model).

3.1 40%-Scaled water model of SEN and mould

3.1.1 Concept design

A few design criteria were laid down before conceptual designs for the 40%-scaled water model were conceived:

- Maximum (laboratory) height restriction of approximately 2 metres

[1] Kinematic viscosity $\nu = \frac{\mu}{\rho}$; μ = dynamic viscosity; ρ = density

- SEN bottom part (nozzle area) must be interchangeable (to easily allow the test of other SEN designs)
- Design should accommodate different widths, ranging from a full-scale 900mm to approximately 1575mm
- Design must share the water source currently used for the existing Columbus tundish water model[2] in the laboratory of the University of Pretoria
- Entire water SEN and mould model must be bolted together, to facilitate easy dismantling in the event of the possible relocation of the water model

The first concept was to use an open tank mounted on top of the SEN/mould to simulate the tundish in the real plant circumstances. According to preliminary calculations, Re-similarity velocities would not be reached (refer to section 3.2 for detailed explanations) owing to the too low Δh due to the height restriction (see Figure 3.1 below).

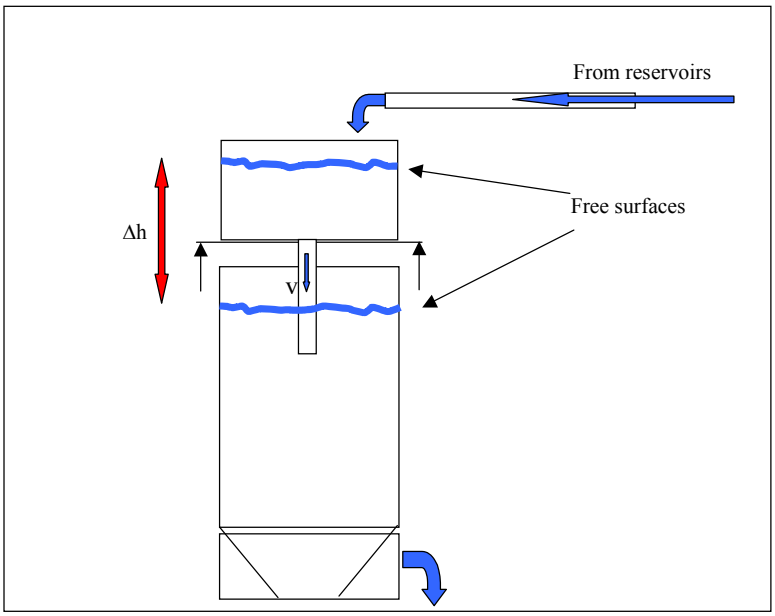

Figure 3.1: Design concept: open tank with Δh as flow velocity source

Calculations proved that a closed top tank would be needed, together with the water reservoirs on the laboratory's roof (currently used for the tundish water

[2] Joint venture by Columbus Stainless, Middelburg, and the cfdlab of the Multi-Disciplinary and Optimisation Group (MDOG), University of Pretoria

model). An additional pump would also be necessary for extra pressure to obtain the correct exit velocity from the SEN ports. Refer to Figure 3.2 for the schematic representation of the final concept and layout of the 40%-scaled water model.

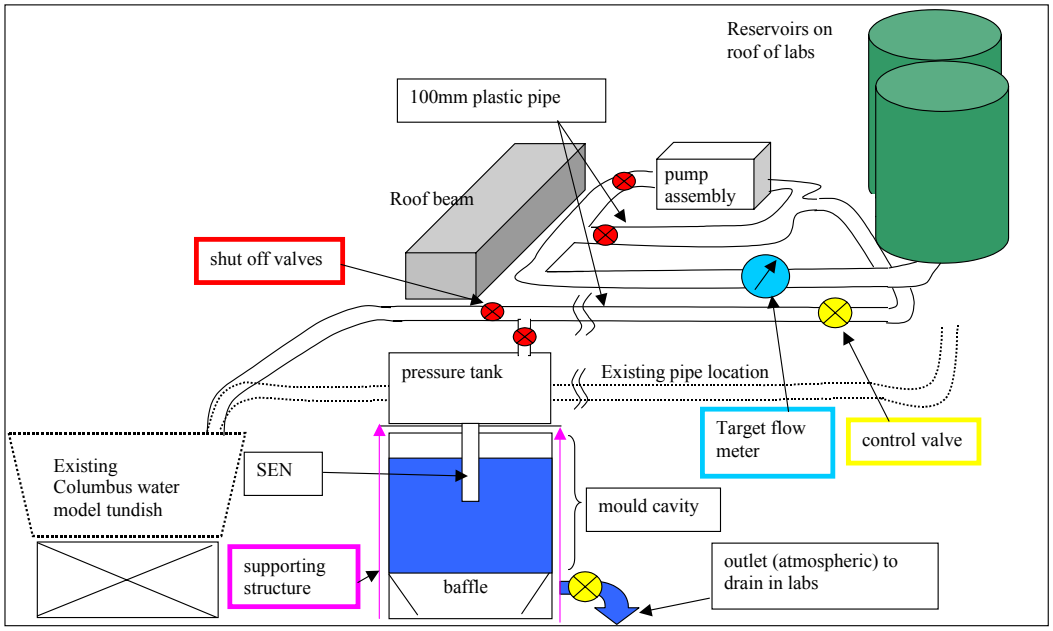

Figure 3.2: Schematic representation of SEN/mould water model and layout

3.1.2 Design

The water model mainly consists of five parts: (Refer to Figure 3.3 for the general water model layout)

1. Top tank with stopper to simulate a tundish. The tank can either be kept open to control the water height, or be closed off to be pressurised for very high flow rates.
2. Perspex mould (not shown in Figure 3.3), which can be varied in width from 360mm to 630mm (a full-scale 900mm to 1575mm). The thickness is a constant 80mm (full-scale 200mm). The thickness can easily be varied at a later stage by installing different narrow Perspex walls.
3. Bottom tank with holes and baffles to slow down and evenly distribute the water flow, together with a gate valve to throttle down the flow towards the drain.

4. Frame that supports the top tank, Perspex mould, as well as the bottom tank.
5. Aluminium SEN consisting of three parts:
    - the upper part connected to the top tank;
    - a middle section which screws onto the upper part;
    - and an insert at the bottom, which contains the bifurcated ports. The insert will typically be the only part that will be altered during SEN design optimisation; consequently costs will be kept low when new optimum designs need to be validated with the water model.

Figure 3.3: General layout of water model (top tank, frame and bottom tank – Perspex mould not shown)

The remaining parts or components mainly consist of pipes, reducers, shut-off valves, elbows, T-sections and other water piping accessories and equipment. These 'off the shelf' components are only applicable to the construction phase (section 3.1.3).

More detail on the design of the five (5) different parts of the water model will follow. Detail design calculations are included in Appendices where deemed necessary.

1. Top tank

Description:

The top tank is constructed from stainless steel and is cylindrically shaped. An inner baffle inside the cylindrical tank, as indicated in Figure 3.4, ensures that the flow simulates the annular flow that typically takes place at the outlet of a tundish. The tank is designed to operate with an open top (for low SEN velocities) or a closed top – where a pressure of at least 6m of water (59kPa gauge) can be accommodated.

As the top tank is not constrained by the rectangular shape of the frame (unlike the bottom tank), the more convenient cylindrical shape saves cost and increases volume.

The thickness of the stainless steel plate used for the tank circumference, inner ring, base and (detachable) lid is 2.5 mm. Calculations showed that 2.5mm thick plate is sufficient to hold the mass of the water, as well as the additional pressure should the faster flow rate be required. Figure 3.4 below shows an isometric view of the upper tank and its detachable lid.

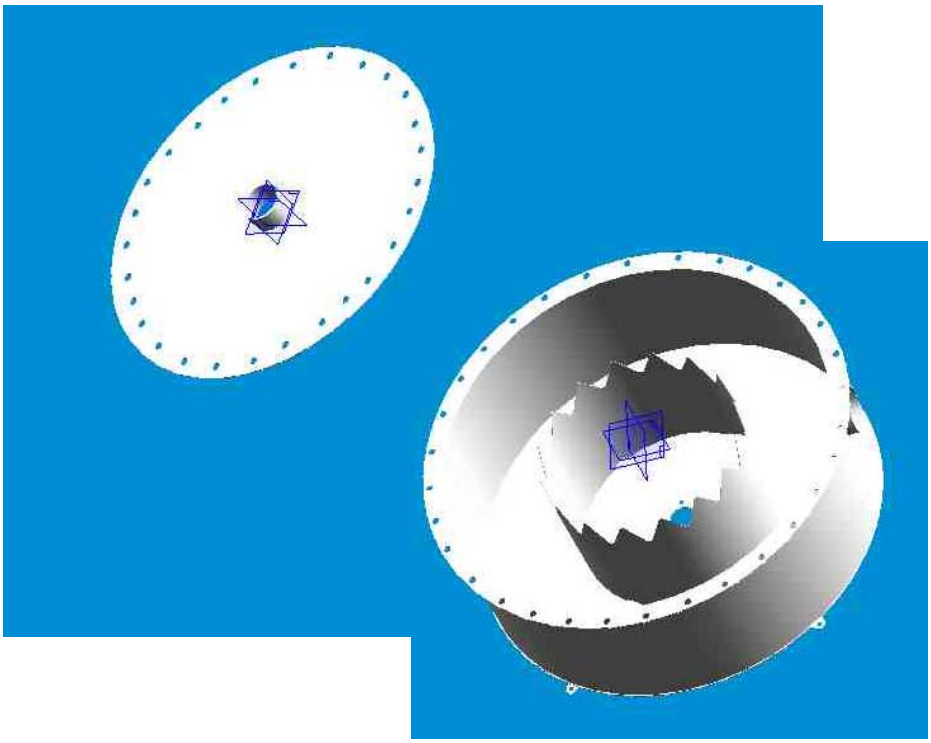

Figure 3.4: Isometric view of upper cylindrical tank and detachable lid

The stopper inside the upper tank can be adjusted to simulate the stopper of a real tundish. Figure 3.5 shows that the stopper can even be adjusted if the lid is fastened, using the extended lead screw. The 40%-scaled stopper has a small hole drilled in its centre, which is connected with a flexible tube to a dye injector (refer to Figure 3.6). A hand drawing (assembly drawing with Aluminium SEN) indicating the dimensions of the 40%-scaled stopper is shown in Appendix D, Figure D.5.

Figure 3.5: Stopper inside the upper cylindrical tank

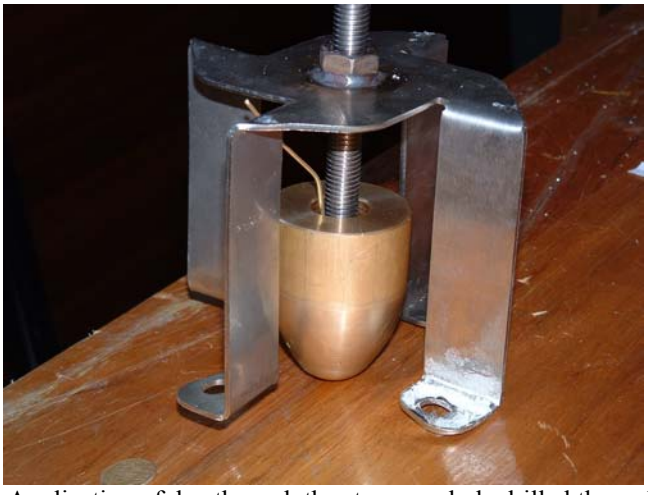

Figure 3.6: Application of dye through the stopper – hole drilled through stopper

2. Perspex mould

The Perspex mould is the most important part of the water model, as the flow visualisation will take place here. In order to maximise visibility, the upper parts of the Perspex mould should not be obscured by steel supports or the frame.

The design is simple, yet different widths (and even slab thicknesses if desired at a later stage) can easily be modelled. Two thick[3] Perspex (Plexiglas) narrow walls are clamped between two Perspex sheets along the length (vertical direction) of the mould cavity using the specifically designed adjustable frame. The four walls (narrow walls and wide walls) are sealed on the bottom tank, also using the frame.

Calculations proved that Perspex with a thickness of 10mm is sufficient to support the worst-case scenario (deepest submergence and largest width), provided the sides are supported throughout the depth, as well as supported in the width at predetermined depths to prevent bulging as the water pressure increases towards the bottom tank.

3. Bottom tank

The bottom tank shape is rectangular in order to be accommodated inside the frame. It is designed from 2.5mm thick stainless steel: the entire tank is designed to be laser-cut, folded and TIG[4] welded. Furthermore, the tank is a sealed unit and cannot be opened. The bottom tank is designed to safely accommodate the pressure exerted by a brim-full mould, as well as sustaining the load of the Perspex mould full of water.

The lid is provided with 16 holes where the Perspex mould is sealed to the bottom tank, to simultaneously slow down the flow. Inside the sealed tank, another three baffles are present in an effort to uniformly slow down the flow towards the exit valve at the bottom of the bottom tank. Refer to Figure 3.7 below for an isometric view of the bottom tank. The baffles inside the tank are not shown, but can be viewed in Appendix B. Also refer to Appendix B for the detail drawings of the bottom tank (open folded sheet metal).

[3] Thick Perspex narrow mould walls: three or four layers of Perspex are bonded or glued together
[4] TIG welding: Tungsten Inert Gas welding. Tungsten tip welding machines are used with an inert gas (mostly CO_2) to weld stainless steel, as high temperatures are required.

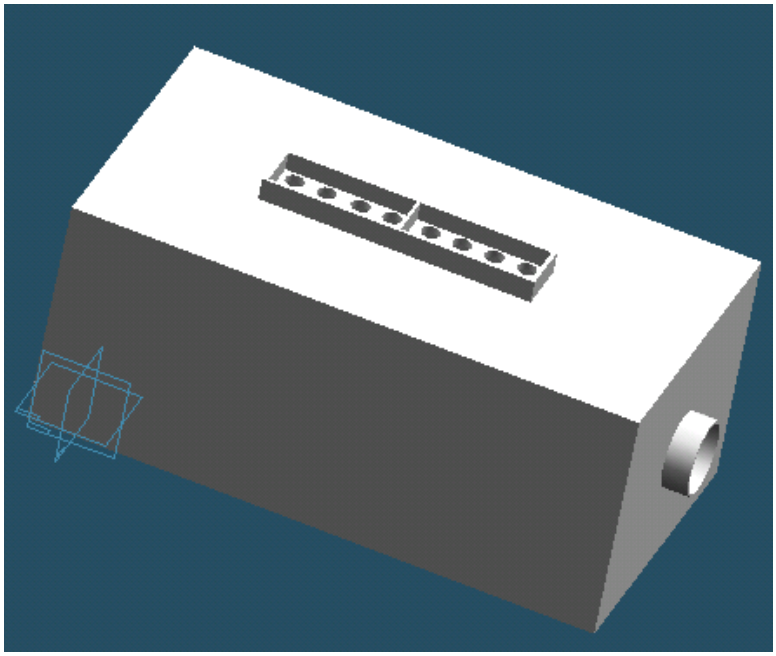

Figure 3.7: Isometric view of bottom rectangular tank (baffles inside not shown)

4. Frame

The fact that the water model must be "portable", implicated that the frame must be able to support itself on a base plate or its own "feet". This ruled out the possibility of erecting a frame that is concreted into the laboratory floor.

The frame concept can be described as four angle iron "legs" bolted onto two similar angle iron feet, separated by quite large section square tubing. (Refer to Figure 3.3 above for clarification). Hanging from the top square tubing separators, four similar square tubing sections ensure that the Perspex walls are pressed firmly against the thin walls, using long bolts and aluminium strips (to distribute the bolt pressure uniformly). These four hanging sections are automatically locked into position due to the outward pressure of the opposing bolts, pressing the Perspex sheets (wide mould walls) against the narrow mould walls.

The steel sections used to construct the frame were chosen after taking into account the mass of the (filled) top water tank, mass of the water inside the Perspex mould, as well as the forces exerted by the hanging sections onto the frame to counter the effect of the water pressure inside the Perspex mould.

Refer to Appendix C for the steel sections chosen (Table C.1). The choice of steel sections was based on not exceeding design stresses (taking into account a Safety Factor of at least 2) caused by bending moments on the sections in question.

Appendix C also shows the final detailed (hand) drawings of the frame and structure, showing where all the sections are utilised.

Mark-off die

During the design phase, the author anticipated potential accuracy problems regarding the connecting holes of the angled sections: a one millimetre mark-off error at the feet or base sections can cause a deviation of more than 200mm at the top of the frame. A special mark-off die was devised to assist in the mark-off procedure, to ensure repeatable and accurate holes in the angled sections.

5. Aluminium SEN

The Aluminium SEN is a 40%-scaled replica of the base case SEN design[5] of Columbus Stainless. The Aluminium SEN consists of three parts.

The insert (bottom part) will typically be the only part that will be altered during SEN design optimisation; consequently costs will be kept low if new optimum designs need to be validated with the water model. Another more inexpensive method of altering the bottom part would be to insert small pieces into a generic bottom part, sealing the bifurcated ports with silicon or something similar.

In order to save time, the Aluminium SEN was manufactured from detail hand drawings. These drawings can be viewed in Appendix D.

[5] Base case SEN design: Refer to Chapter 4 for detail information concerning the current SEN design of the company Columbus Stainless, Middelburg, South Africa. This base case will be the starting design for the optimisation work later in this dissertation, and further work to follow.

The middle section is the most interesting part, which morphs from a circular cross section to a rectangular cross section (including the inside downward ports). A spark erosion technique was used to form the inside ports: a copper mandrel (machined to represent the negative of the inside or downward ports) is connected to large electrical current, causing high-energy sparks (arcing) to the earthed Aluminium SEN. The mandrel slides into the melting Aluminium, forming the desired ports. The manufacturing of these parts was outsourced, as such facilities are not available at the university.

Refer to Figure 3.8 below, which shows the 3 exploded parts of the Aluminium SEN.

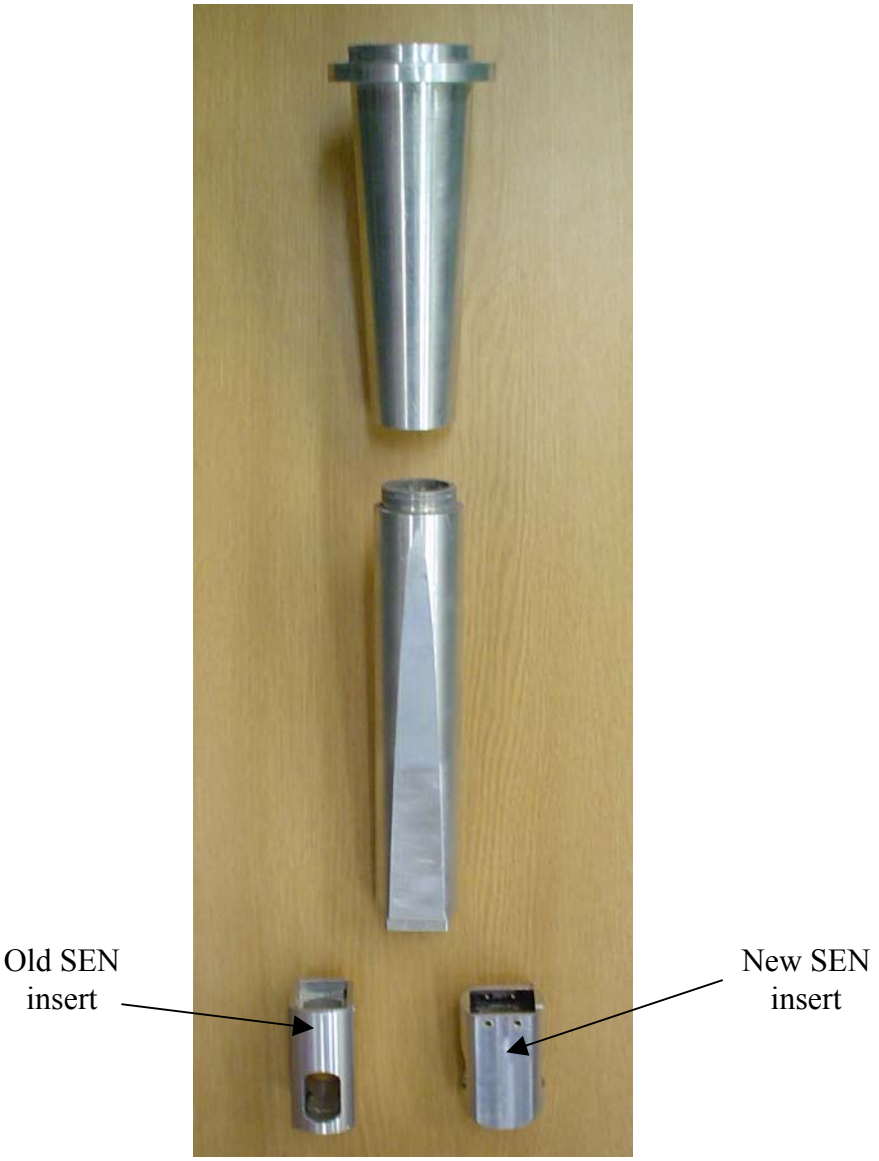

Figure 3.8: Aluminium SEN (3 different parts) shown in exploded view

3.1.3 Construction

In order to avoid elaborate and chronological explanations of the exact progress with regard to the construction of the SEN and mould water model, the construction progress is presented in Appendix E. A Gantt-chart of the progress of the water model construction is also shown for the sake of completeness. Note that the author was involved part-time from January 2003.

3.1.4 Commissioning

Official commissioning took place on 15 September 2003 at the Mechanical Engineering laboratory of the University of Pretoria.

The commissioning could only take place after all pipes, valves and elbows were connected to the water model. The commissioning was performed with an open top tank to enable better view for fault finding, and as only the lower test speeds were to be used.

Figure 3.9 below shows one of the first steps during commissioning, showing water from the nozzle jets exhausting in the air as the Perspex mould is being filled up (by keeping the outlet gate valve at the bottom tank closed).

Figure 3.9: Water model being filled up: SEN nozzles exhausting in the air

The commissioning involved the following tests and actions:

- Fill up the top tank to check for leaks
- Open the stopper in the top tank (refer to Figure 3.5) to enable flow through the SEN
- Keep bottom valve closed until water level is at desired height (thus desired submergence depth for the SEN).
- Check the effectiveness of the seals:
    - between the Perspex mould and bottom tank
    - between the wide mould walls (single Perspex sheet) and the narrow mould walls
- Check for any bulging of the wide walls of the Perspex mould – which will indicate the lack of sufficient support
- Inject dye into the stopper to view the flow patterns. Evaluate the effectiveness of the dye and injection method

The following conclusions were reached after the commissioning, which will be addressed before final and official testing can take place:

- Sealing between Perspex mould and bottom tank inadequate. The use of additional silicon should resolve the matter.
- Sealing between narrow and wide Perspex walls inadequate due to lack of uniform distribution of opposite bolt forces. More aluminium blocks to be used in-between current bolt locations, to distribute sealing forces more uniformly.
- Better flow rate measurements are needed, especially if an open top tank will be used. A rotary flow meter in the outlet of the bottom tank will be installed. If the mould depth is kept constant, the outlet flow meter will accurately represent the flow rate through the SEN.

3.1.5 Further improvements after commissioning

Additional improvements took place since the commissioning of the water model, with the help of an under-graduate student for his fourth year project[6].

The most significant improvements concerned the installation of a rotameter flow meter at the outlet, as well as the replacement of the front Perspex panel with a much stiffer carbon-Perspex sheet. Figure 3.10 shows the upgraded flow control section at the outlet of the mould model.

[6] *Computational and experimental modelling of continuous caster mould and submerged entry nozzle*, Marius Botha, October 2004. Undergraduate thesis, Department Mechanical and Aeronautical Engineering, University of Pretoria.

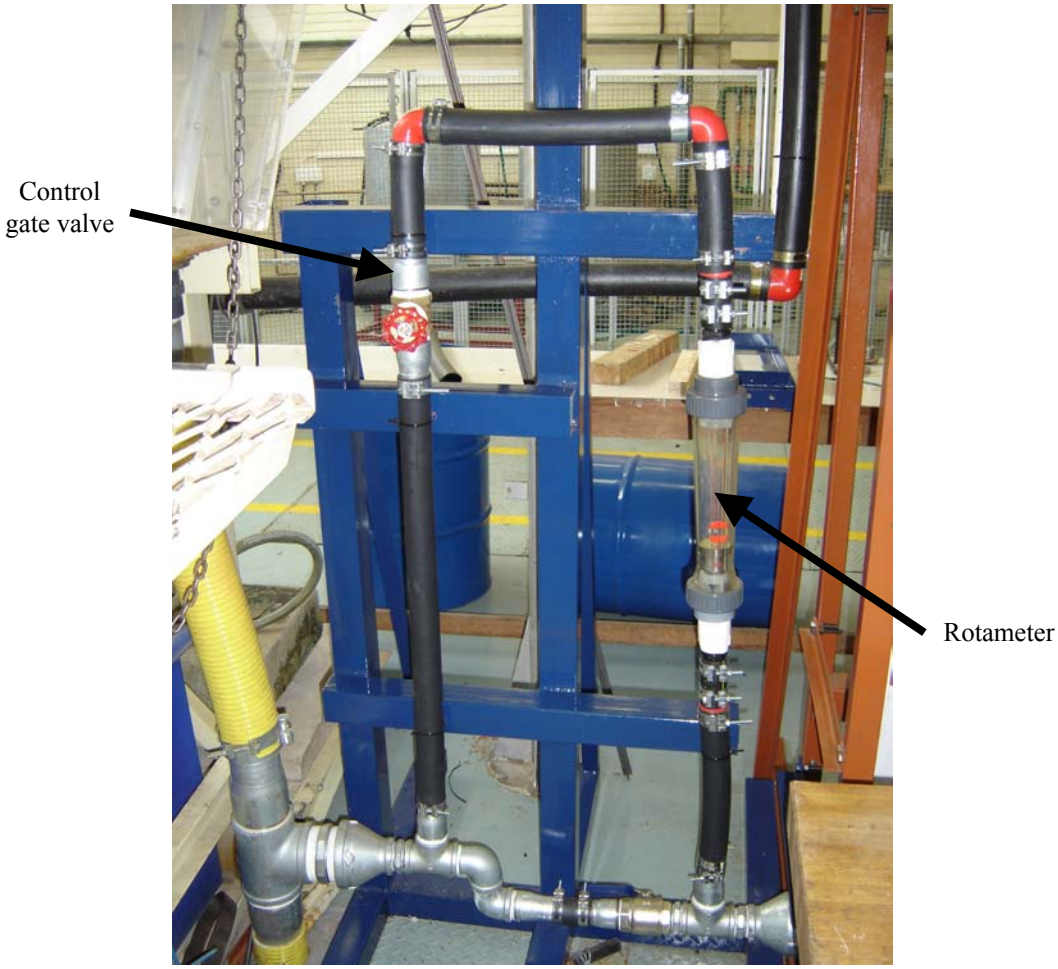

Figure 3.10: Upgraded flow control and flow rate measurement section at the mould model outlet

A modular bottom section of the Aluminium SEN was also devised, consisting of a main body where only small parts or inserts need to be machined. This modular bottom insert is compared with the previous base case bottom insert in Figure 3.11. This is a significant improvement, as the manufacturing of a typical previous bottom section required expensive machining techniques (*i.e.*, spark erosion). The small inserts can be manufactured using conventional milling machines. However, the boxy outside dimensions of the modular bottom section does not correspond exactly to the actual SEN dimensions. However, the effect of these differing outside dimensions on the subsequent flow is assumed to be negligible.

Figure 3.11: Improved modular SEN bottom insert compared with previous insert

Other improvements included:

- General stiffening of the frame (mostly the four hanging pillars exerting pressure onto the Perspex mould)
- Different sealing method: double seal system employing O-rings to seal narrow walls to the wide Perspex walls
- Fixed bolts on hanging pillars to ease set-up of mould during width changes.

3.2 Similarity issues

3.2.1 General

Before comparing results (during and shortly after commissioning) of the 40%-scaled water model with an ADVENT full-scale model [32], some similarity issues need to be elaborated on.

Froude, Reynolds and Weber similarity in scaled modelling

A full-scale water model requires no velocity scaling due to the dynamic similarity between liquid steel and water, as they share approximately the same kinematic viscosity. However, the 40%-scaled model in this dissertation requires a velocity scaling according to Froude, Reynolds or Weber similarity.

Depending on the flow situation, different similarity tests need to be performed:

- If the meniscus motion of the water model needs to be dynamically similar to that of the steel caster, Froude (Fr) similarity needs to be satisfied. The Fr-number relates inertial forces to gravitational forces and is the dominant effect in wave motion of free-surface flows and is totally unimportant if there is no free surface [33].
- If the SEN jet needs to be captured with water modelling tests, Reynolds (Re) similarity should be satisfied. The Re-number is always important, with or without a free surface, as it relates inertial forces to viscous forces, and can be neglected only in flow regions away from high velocity gradients as solid surfaces, jets or wakes.
- Another free-surface parameter is the Weber (Wb[7]) number. It relates inertia to surface tension. The Wb-number is important only if it is of order unity or less, which typically occurs when the surface curvature is comparable in size to the liquid depth, e.g., in droplets, ripple waves and very small hydraulic systems [33].

[7] Some references [9] also make use of the abbreviation We-number when referring to the Weber number.

However, with the assumption that the flow is fully turbulent at a high flow rate, the jet behaviour will be independent of the Re-number and the SEN jet will be dynamically similar at the lower velocity of the Fr-similarity as at the higher flow rate. Refer to section 3.2.3 for detail explanation [33].

3.2.2 Fr-number

The Froude number (Fr-number) is proportional to the ratio of inertial forces to gravitational forces in a flow field or situation. Mathematically, it can be expressed as:

$$Fr = \frac{V^2}{Dg}$$

where: V = velocity
D = diameter or length
g = gravitational constant

As explained above, Fr-similarity needs to be satisfied whenever wave phenomena and meniscus behaviour are modelled. If Fr-similarity is satisfied, the meniscus motion will be dynamically similar to that of the full-scale water model (and therefore the full-scale caster).

In order to compare the 40%-scaled water model meaningfully with a full-scale water model, the flow rate must be calculated to satisfy Fr-similarity.

A typical casting speed is 0.9m/min for a 1575mm-width mould, with a thickness of 200mm.

The plant flow rate (Q_p) will thus be:

$$Q_p = 1.575 \times 0.2 \times \frac{0.9}{60} m^3/s$$

or $Q_p = 17 m^3 / h$

The flow rate for the 40%-scaled model (Q_m) will differ from that of the plant caster. In order to satisfy Fr-similarity, the Fr-numbers must be equal:

$$\frac{V_m^{\ 2}}{D_m g} = \frac{V_p^{\ 2}}{D_p g} \qquad \textbf{[eq 3-1]}$$

where: V_m = velocity inside 40%-scaled model SEN

D_m = diameter or length of 40%-scaled model SEN

g = gravitational constant (9.81 m/s^2)

V_p = velocity inside full-scale SEN

D_p = diameter or length of full-scale SEN

Solving equation 3-1, the necessary velocity of the 40%-scaled model (V_m) can be computed:

$$V_m = \sqrt{\frac{D_m}{D_p}} \times V_p \qquad \textbf{[eq 3-2]}$$

By substituting $D_m/D_p = 0.4$ (**[eq 3-3]**) into equation 3-2, V_m is now expressed in terms of V_p: namely $V_m = 0.632455\ V_p$

Subsequently, the flow rate for the 40%-scaled model, satisfying Fr-similarity, can be expressed as (equation 3-4):

$$Q_m = A_m \times V_m \qquad \textbf{[eq 3-4]}$$

where: Q_m = 40%-scaled model flow rate required

A_m = cross sectional area inside 40%-scaled model SEN

V_m = velocity inside 40%-scaled model SEN

or $$Q_m = \frac{\pi}{4}(D_m^{\ 2}) \times V_m \qquad \textbf{[eq 3-5]}$$

By substituting equation 3-3 into equation 3-5, the following results:

$$Q_m = \frac{\pi}{4}(D_p^{\ 2} \times (0.4)^2) \times 0.632455 V_p \qquad \textbf{[eq 3-6]}$$

Thus, by rearranging equation 3-6,

$$Q_m = \frac{\pi}{4}(D_p^{\,2}) \times V_p \times (0.4)^2 \times 0.632455$$

$$Q_m = A_p \times V_p \times 0.1012$$

Thus: $Q_m = 0.1012 Q_p = 1.72\ \text{m}^3/\text{h}$ **[eq 3-7]**

In order to satisfy Fr-similarity with a 40%-scaled model, a flow rate through the 40%-scaled SEN of approximately 10% of that of the full-scale model or plant caster, is required. Refer to section 3.3 in this chapter to view the results, where the 40%-scaled model is compared with the full-scale model, whilst satisfying Fr-similarity.

3.2.3 Re-number

Re-similarity is regarded as the most important similarity to be adhered to during fluid dynamical scale modelling. The Re-number is proportional to the ratio of inertial forces to viscous forces, and is expressed as

$$\text{Re} = \frac{\rho V D}{\mu}$$

where:
- ρ = density of fluid
- V = velocity
- D = diameter or length
- μ = dynamic viscosity

Following the same process as in section 3.2.2 above, the required flow rate will be calculated in order to satisfy Re-similarity:

Assume that the plant casting speed or flow rate is $Q_p = 17\ \text{m}^3/\text{h}$ again.
In order to satisfy Re-similarity, the corresponding velocity in the 40%-scaled SEN (V_m) must be isolated from equation 3-8 below:

$$\left(\frac{\rho V D}{\mu}\right)_m = \left(\frac{\rho V D}{\mu}\right)_p \qquad \textbf{[eq 3-8]}$$

where: V_m = velocity inside 40%-scaled model SEN

D_m = diameter or length of 40%-scaled model SEN

μ_m = dynamic viscosity of water [1.0×10^{-3} kg/(m.s)

ρ_m = density of water (for water model) [998 kg/m^3]

ρ_p = density of steel (for caster) [6975 kg/m^3]

μ_p = dynamic viscosity of liquid steel [6.4×10^{-3} kg/(m.s)

V_p = velocity inside full-scale SEN

D_p = diameter or length of full-scale SEN

Thus;

$$V_m = \left(\frac{\rho_p \mu_m}{\rho_m \mu_p}\right)\left(\frac{D_p}{D_m}\right) V_p \qquad \textbf{[eq 3-9]}$$

And by substituting the values given in equation 3-8 into equation 3-9, the following is obtained:

$$V_m = (1.092)(2.5) V_p$$
$$= 2.73\ V_p$$

The required flow rate is thus:

$Q_m = \frac{\pi}{4}(D_m^{\,2}) \times V_m$, and following the same process as in section 3.2.2, it follows that

$$Q_m = 0.4368\ Q_p \qquad \textbf{[eq 3-10]}$$

which is approximately 4 times larger than the required flow rate when Fr-similarity is satisfied.

Assumption:

However, as briefly mentioned in the general description above (section 3.2.1), the author assumes that the flow is already fully turbulent at the flow rate corresponding to the Fr-similarity, which renders the jet behaviour independent of the Re-number.

The assumption is vindicated by the following explanation:

Recalling the typical Darcy friction factor[8], f, as a function of the Re-number inside a pipe [33], note that as soon as the flow becomes fully turbulent, f remains constant, independent of the Re-number.

The same principle applies for the flow inside the 40%-scaled SEN and as the jets exit the nozzles: the flow is already fully turbulent when the Fr-similarity is satisfied, as equations 3-11 to 3-12 verifies below.

In order to satisfy Fr-similarity, (from equation 3-7)

$$Q_m = \quad 0.1012\, Q_p \quad = \quad 0.1012(17.01/3600) \quad = \quad 4.7817 \text{ x } 10^{-4} \text{ m}^3/\text{s}$$

The diameter inside the SEN is ϕ24mm (40% of the full-scale ϕ60mm), thus the velocity inside the model is

$$V_m = \frac{Q_m}{A_m} = \frac{4.7817 \times 10^{-4}}{\frac{\pi}{4}(0.024)^2} = 1.057 m/s \qquad \textbf{[eq 3-11]}$$

Using the definition for Re, the Re-number for the 40%-scaled model is calculated:

$$\text{Re} = \frac{\rho V D}{\mu} = \frac{(998)(1.057)(0.024)}{(1 \times 10^{-3})} \approx 25300 \qquad \textbf{[eq 3-12]}$$

For internal flow, fully turbulent flow is assumed at Re ≥ 2300 [9]. The assumption that the flow is already fully turbulent (and thus independent of Re-number) when Fr-similarity is satisfied, is thus plausible.

Table 3.1 below summarises above calculations:

[8] Darcy friction factor: *f*. [33]
This dimensionless parameter is named after Henry Darcy (1803 – 1858), a French engineer renowned for his pipe-flow experiments. *f* is a measure of resistance in a pipe, and is a function of the Re-number and roughness of (the inside of) the pipe. This dimensionless parameter is used for finding primary pipe head loss due to friction using the following equation:

$h_f = f \frac{L}{D} \frac{V^2}{2g}$; L= length of pipe; D = diameter of pipe; V = velocity in pipe; g=9.81 m/s^2

Table 3.1: Summary of Fr-similarity and Re-similarity calculations

	Q_p	Q_m (Fr-similarity)	Q_m (Re-similarity)
Symbols	Q_p	$0.1012Q_p$	$0.4368Q_p$
Base case (0.9m/s cast speed)	17 m^3/h	1.72 m^3/h	7.4256 m^3/h (not applicable due to assumption)

3.2.4 Wb-number

The Wb-number is an important free-surface parameter if it is order unity or less:

$$Wb = \frac{\rho V^2 D}{Y}$$

where: ρ = density of fluid
V = velocity
D = diameter or length
Y = surface tension [water at 20ºC: 0.0728N/m]

In order to verify the influence or sensitivity of the Wb-number, it is evaluated at the flow rate, which satisfies Fr-similarity (V_m=1.057m/s):

$$Wb = \frac{\rho V_m^2 D}{Y} = \frac{(998)(1.057)^2(0.024)}{0.0728} = 367.58 >> 1 \qquad \textbf{[eq 3-13]}$$

In order to investigate the influence of the Wb-number with the (base case) steel caster at a casting speed of 0.9 m/min (corresponding to a flow rate of Q_p = 17 m^3/h), the Wb-number is evaluated using the properties of steel[9]:

$$Wb = \frac{\rho V_m^2 D}{Y} = \frac{(6975)(1.670)^2(0.060)}{0.450} = 2594 >> 1 \qquad \textbf{[eq 3-14]}$$

The Wb-number is sufficiently large for both the 40%-scaled water model and the real steel caster (much larger than unity [33]), and will be neglected for the

[9] The exact surface tension of liquid steel depends on the sulfur content [34]. A value of 450 mN/m proved to be a good average value for typical cast steel.

validation of the 40%-scaled water model. The Wb-similarity will also be neglected in later validations of CFD models (refer to Chapter 4).

3.3 Validation Results and Other Results

For the validation results of the water model verification, there will only be focused on a comparison between the 40%-scaled water model and a full-scale water model.

More detail comparisons between the 40%-scaled water model tests and CFD models, will be expounded on in Chapters 4 and 5. These comparisons will simultaneously *serve* as CFD model verifications. The verification of CFD simulations was and is the main objective of designing and constructing a SEN and mould water model.

3.3.1 Validation of 40%-scaled model with full-scale[10] water model

3.3.1.1 Widest width (1575mm) validation

Figure 3.12 shows the favourable comparison between the 40%-scaled water model with that of the full-scale ADVENT water model [44]. Both water simulations had similar (scaled) submergence depths, identical (scaled) widths, and made use of exactly the same base SEN designs (Columbus Stainless's old design). The flow pattern is made visible by injecting a suitable dye at the top of the SEN (as explained in section 3.1; not shown in Figure 3.12) as soon as the flow is stable and steady (also performed by references [35]). The acceptable correlations prove that the Froude similarity assumption indeed ensures dynamically similar flow fields.

[10] Full-scale model test: performed by ADVENT in 1999. [32]

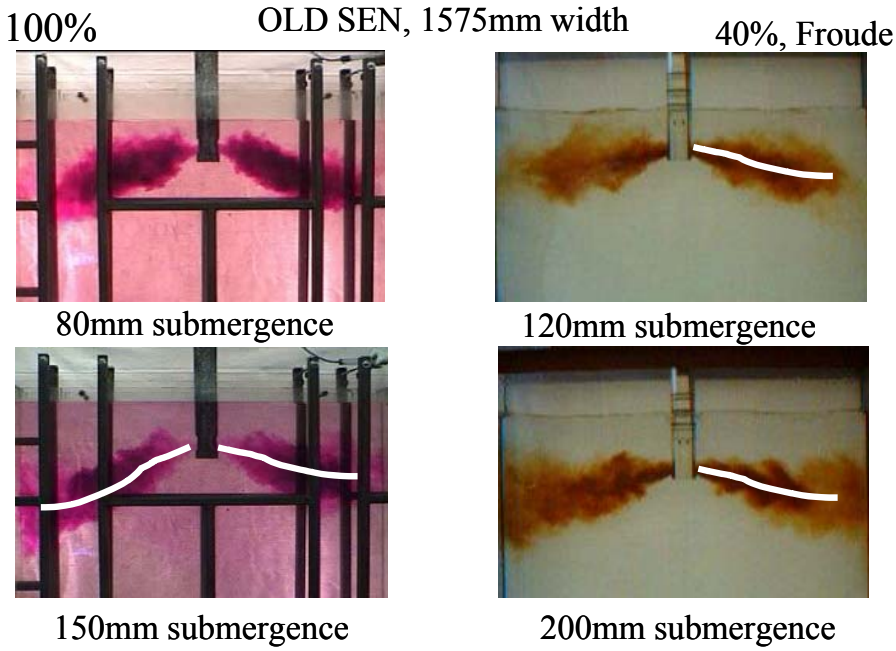

Figure 3.12: Comparison between full-scale ADVENT water model [32] and the 40%-scaled model, satisfying the Fr-similarity in the latter case

The submergence depths, indicated in Figure 3.12, are scaled to the full-scale values. The submergence depth (scaled) values for the two different experiments are not identical, but are regarded to be adequate for preliminary comparison. Refer to Table 3.2 for more detail regarding the two tests.

Table 3.2: Preliminary validation of 40%-scaled water model: comparison with full-scale model

Description	**Full-scale (ADVENT [44])**	**40%-scaled (Preliminary, during commissioning)**
SEN design	Replica of old Columbus SEN	Geometrical identical 40%-scaled
Width of mould	1575mm	630mm (equivalent 1575mm)
Thickness of mould	200mm	80mm (equivalent 200mm)
Flow rate (both experiments)	Q_p = 17 m^3/h	Q_m = 1.72 m^3/h est.[11]. (satisfying Fr-similarity – refer to section 3.2)

[11] This value is estimated as the flow meter during commissioning was not 100% operational

Discussion:

This preliminary comparison enables the reader to just compare the flow patterns made visible by injecting dye. In Chapter 4, with the help of CFD results, more detail on the flow situation will be expounded on.

It is also interesting to note that, especially for the full-scale model, that the flow field is not exactly symmetrical. There can be a number of causes:

- Flow in SEN shaft not uniform. This can result if the water supply is not equivalent to the real plant circumstances.
- SEN ports not exact due to a tolerance issue
- Mould cavity too shallow, which causes unwanted backflow in the upper mould volume, which is not representative of plant circumstances. The full-scale model mould depth is only approximately 1.5 m (which is regarded as too shallow by some references [2]). The 40%-scaled water model has an equivalent full-scale depth in excess of 3m, which is more than sufficient to prevent unwanted backflow interference in the upper mould volume [2].

Furthermore, the relative good correspondence between the 40%-scaled model and the full-scale model confirms that the assumption that the flow is already turbulent at Froude similarity flow velocity (velocity is 40% of full-scale velocity) is correct.

(In order to avoid repetition of explanations, the detail of the flow patterns, differences and similarities will be expounded on in Chapter 4, sections 4.4 to 4.6).

3.3.1.2 Small width (1060mm) validation

Further water model validation tests were also performed on other widths to ensure that the assumption that satisfying Fr-similarity ensures correct jet angles and flow patterns, is correct.

Refer to Figure 3.13 for the validation of the 40%-scaled water model at a (full-scale) submerged depth of 150mm and mould width of 1060mm, satisfying Fr-similarity.

UP 40%-scaled water model **Advent full-scale water model**

Figure 3.13: Comparison between full-scale ADVENT water model [32] and the 40%-scaled model, satisfying Fr-similarity in the latter case: 1060mm mould width

3.3.1.3 Medium width (1250mm) validation

Refer to Figure 3.14 for the validation of the 40%-scaled water model at a (full-scale) submerged depth of 80mm and mould width of 1250mm, satisfying Fr-similarity.

UP 40%-scaled water model **Advent full-scale water model**

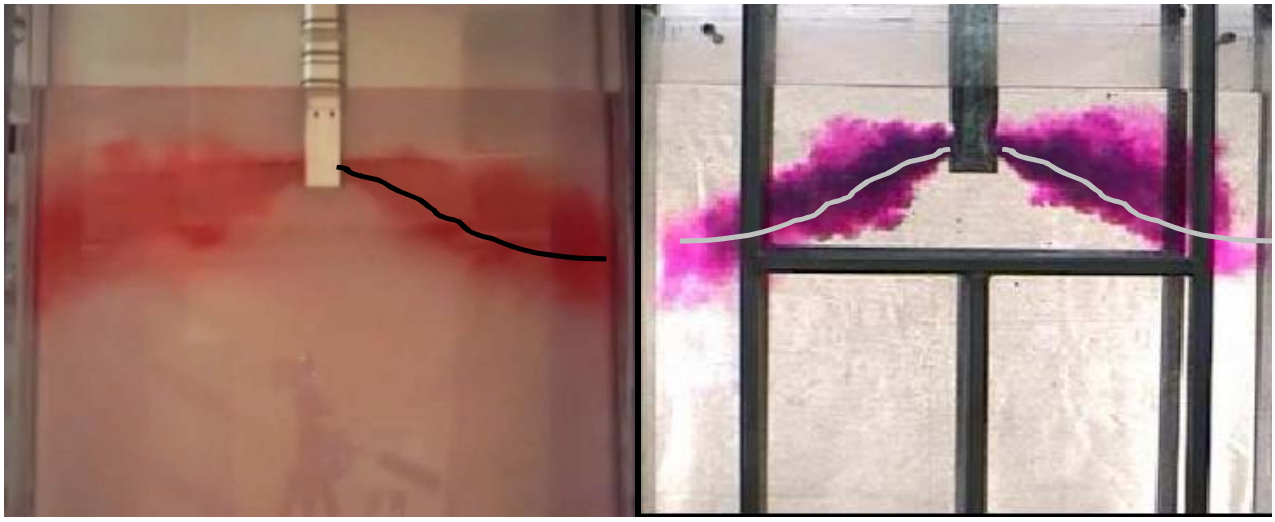

Figure 3.14: Comparison between full-scale ADVENT water model [32] and the 40%-scaled model, satisfying Fr-similarity in the latter case: 1250mm mould width

3.3.2 Other Water Model Results

A number of 40%-scaled water model tests were performed with the two different SEN designs ("old" and "new"[12]) for validation purposes: ultimately, these tests can be used to validate CFD models (in Chapter 4), to ensure physical correctness of these models.

With the water model testing, only the bottom insert of the Aluminium SEN needs to be replaced. (As explained in the design section (section 3.1.2)). Moreover, the new modular SEN bottom section will also be used to perform validation tests of the optimum design achieved in Chapter 5.

All the water model results are displayed in Appendix F.

[12] The old SEN is the original base case SEN design as used by Columbus Stainless. The new SEN design is another case also used in this study for comparison purposes. The exact specifications of the SEN designs are described in Chapter 4. The drawings of the old and new SENs can also be viewed in Appendices G and H respectively.

Two widths will be tested for both SEN designs, each at two different flow speeds (equivalent to casting speeds) and two different submergence depths:

- Widths: 1060mm and 1250mm
- Submergence depths: 80mm and 150mm
- Flow rates
  - 1.28 m^3/h (satisfying Fr-similarity for a casting speed of 1.0 m/min) for 1060mm width
  - 1.52 m^3/h (satisfying Fr-similarity for a casting speed of 1.0 m/min) for 1250mm width

Visualisation:

Although the flow field is assumed to be steady (does not change with passing time), a dye injected into the top of the SEN will highlight the steady flow patterns. However, as the jet mixes with the water in the mould cavity, the jet becomes less visible until the entire mould cavity is the same colour. The double barrel and upward swirling of the jets can also be visualised.

In order to illustrate the three-dimensional flow field, the results will be shown as "snapshots", exactly as the water model test would unfold before an observer.

Discussion:

With reference to Appendix F, the following conclusions are made following the water model results:

Firstly, when similar SEN designs and casting speeds are compared, the jet angle corresponds closely. Consequently, it appears that the submergence depth does not have such a major impact on the jet angle and flow pattern than the SEN design and mould width.

Secondly, a noticeable difference between the old SEN and new SEN is noticed:

The flow pattern of all comparable tests of the old SEN seems much more stable, as opposed to the very fluttering and erratic jet angle (and consequent turning

pattern) of the new SEN. This can be attributed to the design of the new SEN, specifically due to the presence of the well. Refer to Appendix H for the drawings of the new SEN and description of the design. Although the new SEN is not the base case which forms a basic departure point for this study, it is however included for additional information.

Thirdly, the effect of the slightly faster casting speed on each case is quite noticeable. It seems as if the faster jet speed causes a more turbulent (or rather erratic) jet appearance. This fact is theoretically expected, but the visual difference observed was quite unexpected.

The next step towards optimisation of the SEN and mould using CFD techniques is generating CFD models of the base case (or base cases). The 40%-scaled water model, specifically designed and built as described in this chapter, must be used to ensure that the CFD models are physically correct and reliable. As soon as a CFD model can be regarded as trustworthy, optimisation can commence (described extensively in Chapter 5).